COUPLED BEM AND FEM ANALYSIS OF FLUID-STRUCTURE INTERACTION IN DUAL COMPARTMENT TANKS

VASYL V. GNITKO, KYRYL G. DEGTYARIOV, VITALY V. NAUMENKO & ELENA A. STRELNIKOVA*
A.N. Podgorny Institute for Mechanical Engineering Problems of the Ukrainian Academy of Sciences, Ukraine.

ABSTRACT

The paper presents a fluid-structure interaction analysis of fuel tanks with cylindrical and spherical compartments partially filled with a liquid. The compound shell of revolution is considered as a container model. The shell is supposed to be thin, so the Kirchhoff–Love linear theory hypotheses are applied. The liquid is an ideal and incompressible one. Its properties and filling levels may be different within each compartment. The shell vibrations coupled with liquid sloshing under the force of gravity have been considered. The tank structure is modelled by a finite element method, whereas liquid sloshing in the compartments is described by a boundary element method. A system of singular integral equations is obtained for evaluating the fluid pressure. At the first stage, both spherical and cylindrical fluid-filled unconnected rigid shells are considered. Different filling levels as well as small radii of free surfaces are taken into account in problems of liquid sloshing in spherical shells. The sloshing frequencies in the presence of complete or partially covered free surfaces are determined for cylindrical shells. The boundary element method has proven to be effective and accurate in all the problems considered. At the second stage, the natural frequencies and modes of the dual compartment tank are obtained including sloshing, elasticity, and gravity effects.

Keywords: baffles, boundary and finite element methods, fluid-structure interaction, free vibrations, fuel tanks, sloshing

1 INTRODUCTION

The low frequency oscillations of free surfaces in partially filled containers significantly increase dynamic responses of structures containing liquids. This phenomenon is known as sloshing. It can result in severe structural damage, loss of stability, and failure.

In order to suppress sloshing, a variety of methods have been proposed, simulated, and tested. The boundary element method (BEM) has been successfully used in solution of both linear and non-linear sloshing problems. In order to solve the large-scale problems, researchers developed the multi-domain boundary element method (MBEM). The multi-domain collocation strategy was briefly introduced by Brebbia *et al.* [1] and then developed by Wang and Gao [2]. The MBEM is especially effective if the computational domain has a complicated structure. It is successfully applied for numerical simulation of sloshing in multi-compartment fuel tanks with different types of baffles.

The effect of baffles on sloshing frequencies was studied by Biswal *et al.* [3]. The numerical method using a finite element formulation was developed by Kumar and Sinhamahapatra [4] to analyze dynamic effects of perforated vertical baffles. Sloshing in spherical tanks for liquefied natural gas carriers was studied by Faltinsen and Timokha [5] and for water supply towers by Curadelli *et al.* [6]. Ravnik *et al.* [7] presented a fluid-structure interaction analysis of the cylindrical fuel tank with two compartments partially filled with a liquid. But fluid-structure interaction problems for fuel tanks of more complicated shapes are still not fully described in the literature.

ORCID: http://orcid.org/0000-0003-0707-7214

2 PROBLEM STATEMENT

In this paper, we describe applications of multi-domain and single-domain boundary element methods to the fluid-structure interaction analysis of compound fuel tanks.

Consider a fuel tank with cylindrical and spherical compartments. The internal baffles can be installed in both compartments for slosh suppression. The structure and its sketch are shown in Fig. 1.

Assume that both compartments are partly filled with an incompressible ideal liquid. Fluid motion is considered to be irrotational.

Suppose σ is a wetted part of the structure surfaces, S_{01} and S_{02} are free surfaces of the liquid in spherical and cylindrical compartments, respectively. Let S_0 be $S_0 = S_{01} \cup S_{02}$. The wetted surface σ consists of four parts, namely, $\sigma = S_{w1} \cup S_{w2} \cup S_{bot} \cup S_{baf}$. Here S_{w1} and S_{w2} are the wetted surfaces of cylindrical and spherical parts, S_{bot} is a bottom surface of the tank and S_{baf} is a baffle surface. The domains occupied with the liquid are denoted by Σ_1 and Σ_2 for cylindrical and spherical compartments, respectively. Let $\Sigma_{12} = \partial\Sigma_1 \cap \partial\Sigma_2$ be the common part of wetted surface areas. The liquid densities are ρ_1 and ρ_2, and filling levels are h_1 and h_2 in Σ_1 and Σ_2, respectively. Let R_{ir} be the inner radius of the ring free surface (Fig. 1).

Consider at first free vibrations of the empty elastic shell structure. Assume that a time dependent vector of the shell displacements $\tilde{\mathbf{U}}$ is given by

$$\tilde{\mathbf{U}} = \tilde{\mathbf{u}}\exp(i\Omega t); \quad \tilde{\mathbf{u}} = (u_1, u_2, u_3),$$

where Ω is a vibration frequency. The time factor $\exp(i\Omega)$ will be omitted further on. After separation of the time factor, the shell vibrations are described by the system of three partial differential equations

$$\sum_{i=1}^{3} L_{ij}u_i = \Omega^2 u_j, \quad j = 1,2,3,$$

where L_{ij} are linear differential operators of the Kirchhoff–Love shell theory described by Wan *et al.* [8]. To obtain the natural frequencies Ω_k and modes $\mathbf{u}_k (k = 1, N)$ of the shell structure, the finite element method is applied [7].
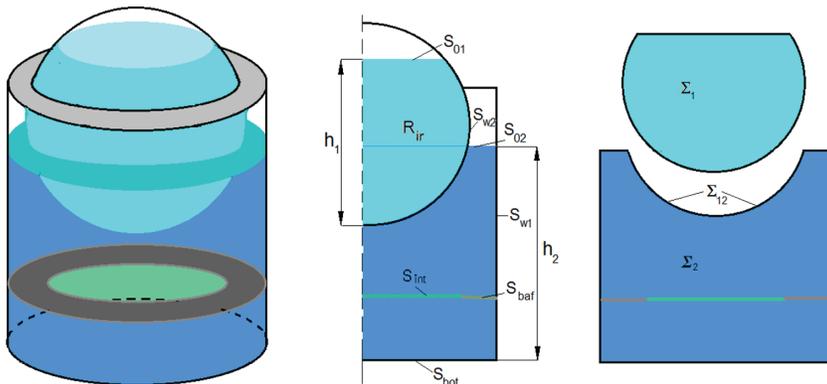
Figure 1: Shell structure with an internal baffle, its sketch and fluid subdomains.

Let $\mathbf{U}=(U_1,U_2,U_3)$ be displacements of the fluid-filled elastic shell structure. After forming the global stiffness and mass matrices $\mathbf{L}$ and $\mathbf{M}$, the following equation of motion for the tank filled with the liquid has been obtained [7]:

$$\mathbf{LU} + \mathbf{M\ddot{U}} = \mathbf{P}. \tag{1}$$

Here $\mathbf{P}$ gives the fluid dynamical pressure onto the shell structure normal to its surface.

Assuming the flow to be inviscid and irrotational, the incompressible fluid motion in the 3D tank is described by the Laplace equation

$$\nabla^2\Phi = 0, \tag{2}$$

where Φ is a velocity potential.

To determine this potential a mixed boundary value problem for the Laplace equation is formulated in the double domain $\Sigma_1 \cup \Sigma_2$. The non-penetration condition on the wetted tank surfaces σ is following:

$$\left.\frac{\partial\Phi}{\partial\mathbf{n}}\right|_\sigma = \frac{\partial w}{\partial t}. \tag{3}$$

Here $\mathbf{n}$ is an external unit normal to the tank wetted surfaces, w denotes a normal component of the displacement vector $\mathbf{U}$, namely, $w = (\mathbf{U},\mathbf{n})$. Let functions $\varsigma_1(t,x,y)$ and $\varsigma_2(t,x,y)$ be free surface elevations in the first and second compartments (Fig. 1). By p_i denote the pressure on the free surfaces $S_{0i}(i=1,2)$. Let p_0 be an atmospheric pressure. Then the kinematic and dynamic boundary conditions on S_{01} and S_{02} can be expressed as follows:

$$\left.\frac{\partial\Phi}{\partial\mathbf{n}}\right|_{S_{0i}} = \frac{\partial\zeta_i}{\partial t}; \quad p_i - p_0|_{S_{0i}} = 0; \quad i=1,2, \tag{4}$$

On the free surfaces, the following formulae for p_i ($i=1,2$) are valid:

$$p_1 - p_0 = -\rho_1\left.\left(\frac{\partial\Phi}{\partial t} + g\zeta_1\right)\right|_{S_{01}}; \quad p_2 - p_0 = -\rho_2\left.\left(\frac{\partial\Phi}{\partial t} + g\zeta_2\right)\right|_{S_{02}}.$$

Here g is the gravity acceleration.

Denote by $\Phi^{(i)}$ values of the velocity potential Φ at points $P \in \partial\Sigma_i$ $(i=1,2)$.

Equations (1) and (2) are solved simultaneously using the shell fixation conditions relative to $\mathbf{U}$, boundary conditions (3) and (4), and the following expressions for dynamical components of the liquid pressure on elastic walls:

$$p_l = (\mathbf{P},\mathbf{n}) = \begin{cases} -\rho_1\dfrac{\partial\Phi^{(1)}}{\partial t}; & P \in S_{w1}\bigcup S_{\text{bot}}; \\[2mm] -\rho_2\dfrac{\partial\Phi^{(2)}}{\partial t}; & P \in S_{w2}\setminus\Sigma_{12}; \\[2mm] -\left(\rho_1\dfrac{\partial\Phi^{(1)}}{\partial t} - \rho_2\dfrac{\partial\Phi^{(2)}}{\partial t}\right); & P \in \Sigma_{12}. \end{cases}$$

To define modes of shell vibrations coupled with liquid sloshing, we will represent displacements of the fluid-filled tank as $\mathbf{U}=\mathbf{u_f}\times\exp(i\omega t)$. Here ω and $\mathbf{u_f}$ are natural frequencies and vibration modes of the fluid-filled shell structure.

3 THE MODE SUPERPOSITION METHOD FOR COUPLED DYNAMIC PROBLEMS

Consider the vibration modes of the fluid-filled tank in a form

$$\mathbf{U} = \sum_{k=1}^{N} c_k \mathbf{u}_k, \tag{5}$$

where $c_k = c_k(t)$ are unknown coefficients, and $\mathbf{u}_k$ are eigenmodes of the empty tank. In other words, the mode of vibration of the fluid-filled tank is determined as a linear combination of eigenmodes of the empty shell structure. Note that the following relationships are fulfilled [7]

$$\mathbf{L}(\mathbf{u}_k) = \Omega_k^2 \mathbf{M}(\mathbf{u}_k), \quad (\mathbf{M}(\mathbf{u}_k), \mathbf{u}_j) = \delta_{kj}. \tag{6}$$

Hence

$$(\mathbf{L}(\mathbf{u}_k), \mathbf{u}_j) = \Omega_k^2 \delta_{kj}, \tag{7}$$

where Ω_k is the k-th frequency of the empty tank vibrations. Equations (6) and (7) show that the abovementioned vibration modes have to be orthonormalized with respect to the mass matrix.

Let also introduce $\mathbf{u}_k^i$ as follows:

$$\mathbf{u}_k = \begin{cases} \mathbf{u}_k^1; & P \in \Sigma_1, \\ \mathbf{u}_k^2; & P \in \Sigma_2. \end{cases}$$

Consider Φ as a sum of two potentials $\Phi = \Phi_1 + \Phi_2$ as it was done by Degtyarev *et al.* [9]. Represent potential Φ_1 as the following series:

$$\Phi_1 = \sum_{k=1}^{N} \dot{c}_k(t) \phi_{1k}. \tag{8}$$

Here the time-dependant coefficients $c_k(t)$ are defined in eqn (5). To determine functions φ_{1k} $\left(k = \overline{1,N}\right)$, we have the following boundary value problems:

$$\nabla^2 \phi_{1k}^i = 0; \quad P \in \Sigma_i; \left.\frac{\partial \phi_{1k}^i}{\partial \mathbf{n}}\right|_{S_{wi}} = w_k^i; \left.\frac{\partial \phi_{1k}^1}{\partial \mathbf{n}}\right|_{S_{bot}} = w_k^i; \left.\phi_{1k}^i\right|_{S_{i0}} = 0. \tag{9}$$

Here, w_k^1, w_k^2 are normal components of the mode $\mathbf{u}_k$ in the first and second compartments, $w_k^i = \left(\mathbf{u}_k^i, \mathbf{n}\right)$. So functions ϕ_{1k}^1 and ϕ_{1k}^2 are solutions of problems (9) for $i = 1$ and $i = 2$, accordingly, as in Ref. [10].

To determine potential Φ_2, we must solve the boundary value problems of fluid vibrations in two disconnected compartments with rigid walls. These problems are solved separately for spherical and cylindrical parts. To obtain the sloshing modes, the following sequence of boundary value problems for auxiliary functions ψ_{2k}^i $\left(i = 1,2\right)$ is formulated:

$$\Delta \psi_{2k}^{i} = 0; \quad \left. \frac{\partial \psi_{2k}^{i}}{\partial \mathbf{n}} \right|_{S_{wi}} = 0; \quad \left. \frac{\partial \psi_{2k}^{1}}{\partial \mathbf{n}} \right|_{S_{bot}} = 0;$$

$$\left. \frac{\partial \psi_{2k}^{i}}{\partial \mathbf{n}} \right|_{S_{0i}} = \frac{\partial \varsigma_i}{\partial t}; \quad \left. \frac{\partial \psi_{2k}^{i}}{\partial t} + g\zeta_i \right|_{S_{0i}} = 0, \, k = \overline{1,N}; \quad i = 1,2.$$

Suppose hereinafter $\psi_{2k}(t,x,y,z) = e^{i\chi_k t} \phi_{2k}(x,y,z)$. Then we obtain the following eigenvalue problems [9, 10] for each ϕ_{2k}^{i} $(i = 1,2)$ in the liquid domains $\Sigma_i (i = 1,2)$:

$$\Delta \phi_{2k}^{i} = 0 \Big|_{\Sigma_i}; \left. \frac{\partial \phi_{2k}^{i}}{\partial \mathbf{n}} \right|_{S_{wi}} = 0; \left. \frac{\partial \phi_{2k}^{1}}{\partial \mathbf{n}} \right|_{S_{bot}} = 0; \left. \frac{\partial \phi_{2k}^{i}}{\partial \mathbf{n}} = \frac{\chi_k^2}{g} \phi_{2k}^{i} \right|_{S_{0i}}; \int_{S_{0i}} \phi_{2k}^{i} dS = 0. \tag{10}$$

So for potentials Φ_1 and Φ_2 we obtain the next representations:

$$\Phi_1 = \begin{cases} \sum_{k=1}^{M_1} c_k \phi_{1k}^{1}, & P \in \Sigma_1, \\ \sum_{k=1}^{M_2} c_k \phi_{1k}^{2}, & P \in \Sigma_2, \end{cases} ; \Phi_2 = \begin{cases} \sum_{k=1}^{L_1} \dot{d}_k \phi_{2k}^{1}, & P \in \Sigma_1, \\ \sum_{k=1}^{L_2} \dot{d}_k \phi_{2k}^{2}, & P \in \Sigma_2. \end{cases} \tag{11}$$

Here $c_k(t), d_k(t)$ are unknown time-dependant coefficients.

The effective numerical procedure for solution of eigenvalue problems (10) using the single and multi-domain boundary element methods has been introduced in Refs. [7, 10].

Thus, the problem under consideration involves the following steps. First, it is necessary to obtain the sloshing frequencies and modes ϕ_{2k}^{i} using rigid wall assumption. Second, we obtain the natural frequencies Ω_k and modes $\mathbf{u}_k$ of the empty elastic tank. Then we define the free vibration frequencies and modes ϕ_{1k}^{i} of the elastic tank without considering effects of sloshing. When functions ϕ_{1k}^{i} and ϕ_{2k}^{i} are defined, we substitute them in eqns (11) and (1) and obtain the system of ordinary differential equations as it was done in Ref. [10]. Finally, the flow-induced vibrations of elastic structures are studied.

To define functions ϕ_{1k}^{i} and ϕ_{2k}^{i} we use the boundary element method in its direct formulation [1]. Dropping indices i, $1k$ and $2k$ one can obtain the main integral equation in the following form:

$$2\pi\phi(P_0) = \iint_S q \frac{1}{|P - P_0|} dS - \iint_S \phi \frac{\partial}{\partial \mathbf{n}} \frac{1}{|P - P_0|} dS. \tag{12}$$

Here, $S = \sigma \cup S_0$, points P and P_0 belong to the surface S. The value $|P - P_0|$ represents Cartesian distance between the points P and P_0. In doing so, the function φ defined on the wetted tank surface σ presents the pressure, and the function q defined on the free surface S_0, is the flux, $q = \partial\phi / \partial\mathbf{n}$. To apply the MBEM, we introduce the artificial interface surface S_{int} [11]–[12]. In MBEM, the computational domain is divided into a number of subdomains, and the BEM algebraic equations are established for each subdomain. Then the global system of algebraic equations is formed by assembling results of all subdomains in terms of the equilibrium and matching conditions over common interface nodes. This system has a blocked and sparse character.

The basic procedure is to start with the standard boundary integral equation for potential (12), replace Cartesian coordinates (x, y, z) with cylindrical ones (r, θ, z), and integrate with respect to z and θ. We use furthermore the cylindrical coordinate system, and represent unknown functions as Fourier series by the circumferential coordinate θ

$$w_k^i(r,z,\theta) = w_k^i(r,z)\cos\alpha\theta; \quad \phi_{jk}^i(r,z,\theta) = \phi_{jk}^i(r,z)\cos\alpha\theta; \ i=1,2; \ j=1,2; \ k=1,2,..., \ (13)$$

where α is a given integer (the number of nodal diameters). In this case, the solution is independent of the angular coordinate θ, and the three-dimensional problem is reduced to a two-dimensional one in the radial coordinate r and the axial coordinate z.

Let Γ be a generator of the surface σ. Using (12), (13) we have obtained the following system of singular integral equations for unknown functions φ and q in problem (9):

$$2\pi\phi(z_0) + \int_\Gamma \phi(z)Q(z,z_0)r(z)d\Gamma - \int_0^R q(\rho)\Psi(P,P_0)\rho d\rho = \int_\Gamma w(z)\Psi(P,P_0)r(z)d\Gamma_1; P_0 \in \sigma;$$

$$\int_\Gamma \phi(z)Q(z,z_0)r(z)d\Gamma - \int_0^R q(\rho)\Psi(P,P_0)\rho d\rho = \int_\Gamma w(z)\Psi(P,P_0)r(z)d\Gamma_1; \ P_0 \in S_0.$$

Here

$$Q(z,z_0) = \frac{4}{\sqrt{a+b}}\left\{\frac{1}{2r}\left[\frac{r^2 - r_0^2 + (z_0 - z)^2}{a-b}\mathsf{E}_\alpha(k) - \mathsf{F}_\alpha(k)\right]n_r + \frac{z_0 - z}{a-b}\mathsf{E}_\alpha(k)n_z\right\};$$

$$\Psi(P,P_0) = \frac{4}{\sqrt{a+b}}\mathsf{F}_\alpha(k); \ \mathsf{E}_\alpha(k) = (-1)^\alpha(1-4\alpha^2)\int_0^{\pi/2}\cos 2\alpha\psi\sqrt{1-k^2\sin^2\psi}\,d\psi;$$

$$\mathsf{F}_\alpha(k) = (-1)^\alpha\int_0^{\pi/2}\frac{\cos 2\alpha\psi\,d\psi}{\sqrt{1-k^2\sin^2\psi}}; \ a = \rho^2 + \rho_0^2 + (z-z_0)^2; \quad b = 2\rho\rho_0; k^2 = \frac{2b}{a+b}.$$

The system of singular integral equations for mixed boundary value problem (10) has been obtained in Ref. [10]. Numerical procedures to solve these problems based on the boundary element method are described in details in the papers [7, 9, 11].

4 SOME NUMERICAL RESULTS

4.1 Low frequency sloshing modes for partially filled spherical shells

4.1.1 Spherical shells without baffles
Now we turn to the problem of sloshing in the spherical container without baffles. Radius of the sphere is R_1=1m; the filling level is h_1.

The numerical simulation has been provided for different values of h_1 $(0.2 < h_1 / R_1 < 1.99)$ and different modes a $(\alpha = \overline{0,3})$. Both SBEM and MBEM are applied here. The boundary elements with constant approximation of unknowns inside elements are used. In SBEM there are 200 elements along the spherical surface and 150 elements along the free surface. In MBEM we divide the computational domain into two parts by an artificial interface surface at $h_{\text{int}} = 0.5h_1$ using 100 boundary elements in each subdomain along the spherical surface and 150 elements along the free surface.

We use practically the same mesh to find a numerical approximation of low eigenvalues for the so-called 'ice-fishing problem'. In this problem, formally, we should consider an infinitely wide and deep ocean covered with ice, with a small round fishing hole. Sloshing in such 'containers' was studied by McIver [12]. We approximate this infinite case using the spherical tank with the small round hole on its top. It allows us to compare our numerical results with those obtained in the papers [12–14].

Proposed boundary element approach gives nearly the same values as the other authors. In Tables 1 and 2 we compare our results obtained by using SBEM and MBEM with those obtained in Refs. [12–14] for axisymmetric ($a = 0$) and non-axisymmetric ($a = 1$) modes. Four first frequencies ($m = 1, 4$) are evaluated for each a. Here we consider different filling levels h_1. The value $h_1/R_1 = 1.99$ corresponds to the ice-fishing problem. The results of Faltinsen and Timokha [13], and Kulczycki *et al.* [14] are very close. Both Refs. [13–14] and [12] results analytically approximate the sloshing eigenvalues of the spherical tank.

It should be noted that results obtained by SBEM are more precise than MBEM ones, but the matrix size in SBEM is twice larger compared with MBEM. If un-baffled tanks are at low filling levels, it is preferable to use SBEM. The numerical analysis demonstrates that the lowest liquid sloshing frequency occurs for mode $a = 1$.

Considering our approximate natural sloshing modes one can observe how free surface profiles change with the liquid depth. These results are illustrated in Fig. 2 for the three lowest eigenvalues of the mode $a = 1$. Here numbers 1, 2, 3, 4 correspond to the different non-dimensional filling levels: $h_1/R_1 = 1.0$; 0.2; 1.8; 1.9, respectively.

In the spherical tank with $0 < h_1/R_1 < 0.5$ the lowest mode presents a spatial wave pattern that look like inclination of an almost flat free surface. Increasing the liquid depth yields more

Table 1: Axisymmetric slosh frequencies of the fluid-filled spherical shell, Hz.

m	Method	Filling level h_1, m				
		$h_1 = 0.2$	$h_1 = 0.6$	$h_1 = 1.0$	$h_1 = 1.8$	$h_1 = 1.99$
1	[13,14],	3.8261	3.6501	3.7451	6.7641	29.0500
	[12]	3.8261	3.6501	3.7451	6.7641	29.2151
	MBEM	3.4034	3.5455	3.7294	6.6098	30.7081
	SBEM	3.8314	3.6510	3.7456	6.7665	29.1811
2	[13,14],	9.2561	7.2659	6.9763	12.1139	51.8122
	[12]	9.2561	7.2659	6.9763	12.1139	52.0467
	MBEM	9.2636	7.2893	6.9796	12.0008	52.9393
	SBEM	9.2686	7.2684	6.9780	12.1205	52.0255
3	[13,14],	14.7556	10.7443	10.1474	17.3960	74.2909
	[12]	14.7556	10.7443	10.1474	17.3960	74.5537
	MBEM	14.9214	10.7483	10.1496	17.3136	75.3139
	SBEM	14.7763	10.7502	10.1512	17.4086	74.5547
4	[13,14],	20.1187	14.1964	13.3041	22.6579	96.6207
	[12]	20.1187	14.1964	13.3041	22.6570	96.9560
	MBEM	20.2066	14.2023	13.3083	22.5962	97.7771
	SBEM	20.1498	14.2056	13.3110	22.6777	96.9021

Table 2: Non-axisymmetric slosh frequencies of the fluid-filled spherical shell, Hz.

m	Method	Filling level h_1, m				
		$h_1 = 0.2$	$h_1 = 0.6$	$h_1 = 1.0$	$h_1 = 1.8$	$h_1 = 1.99$
1	[13,14],	1.0723	1.2625	1.5601	3.9593	18.9838
	[12]	1.0723	1.2625	1.5601	3.9593	19.1582
	MBEM	1.1034	1.2777	1.5638	3.9606	19.1603
	SBEM	1.0723	1.2626	1.5603	3.9508	19.1130
2	[13,14],	6.2008	5.3860	5.2755	9.4534	41.3491
	[12]	6.2008	5.3860	5.2755	9.4534	41.7683
	MBEM	6.1227	5.3534	5.2749	9.4582	41.5327
	SBEM	6.2090	5.3697	5.2764	9.4538	41.5333
3	[13,14],	11.8821	8.9418	8.5044	14.7548	63.5354
	[12]	11.8821	8.9418	8.5044	14.7548	64.0323
	MBEM	11.9650	8.9529	8.5062	14.7648	63.9483
	SBEM	11.8981	8.9429	8.5069	14.7574	63.8783
4	[13,14],	17.3581	12.4234	11.6835	20.0224	85.9166
	[12]	17.3584	12.4234	11.6835	20.0224	86.3001
	MBEM	17.4540	12.4276	11.6863	20.0394	86.2972
	SBEM	17.3842	12.4291	11.6884	20.0278	86.2034

complicated free surface profiles. Figure 3 demonstrates the spatial wave patterns for $a = 1$, $m = 1, 2, 3$ at $h_1/R_1 = 1.8$.

4.1.2 Spherical shells with baffles
Consider the rigid spherical tank of radius $R_1 = 1$ m filled to the depth $h_1 = 1.4$ m. The inner periphery of the tank contains a thin rigid-ring baffle. The baffle position is $h_{baf} = 1$ m. The different annular orifices in the baffle are considered. Radii of these orifices are radii R_{int} of the interface surfaces. The first four frequencies for mode $a = 1$ are evaluated for radii $R_{int} = 1.0$ m, $R_{int} = 0.7$ m, and $R_{int} = 0.2$ m. Note that $R_{int} = 1.0$ m correspond to the un-baffled tank. The frequencies are presented in Table 3.

The results show that frequencies decrease as radius of the baffle orifice is decreased. Only the lowest eigenvalue is essentially influenced by installing the baffles.

Figure 4 demonstrates the first non-axisymmetric modes of liquid vibrations in spherical tanks with and without baffles. When the baffle is installed, the mode shape becomes almost flat.

4.2 Sloshing frequencies for partially filled cylindrical tanks with covered free surfaces

Consider eigenvalue problem (10) for the second fluid domain Σ_2 bounded by cylindrical and spherical surfaces (Fig. 1). By H denote a height of the cylinder, by R_1, R_2 radii of the spherical and cylindrical parts, and by h_2 the filling level in Σ_2. Let $(0, z_s)$ be centre coordinates of the sphere. The shell structure has following dimensions: $R_1 = 1$ m; $R_2 = 1.2$ m; $z_s = 1.5$ m; $H = 2.$m. The modes and frequencies are evaluated for different h_2 in the range of
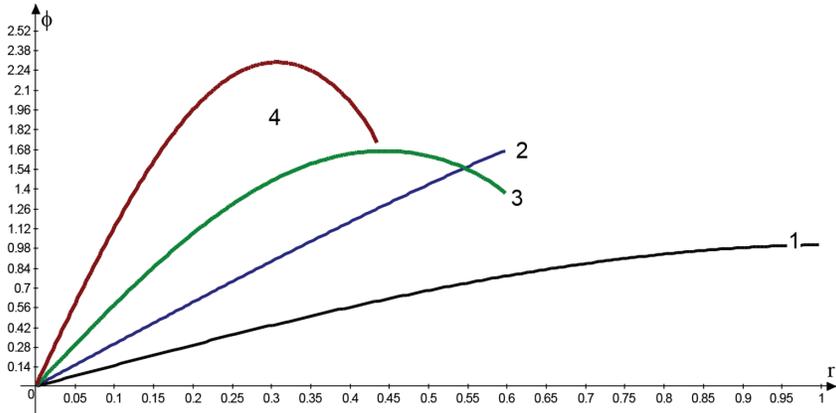
a) $\alpha = 1$, $m=1$
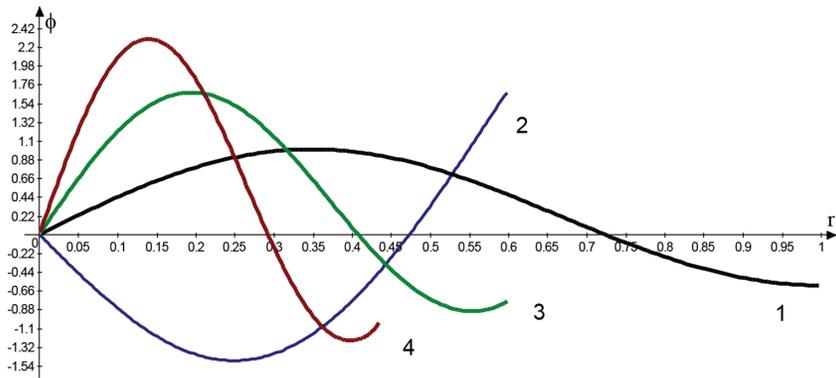
b) $\alpha = 1$, $m=2$
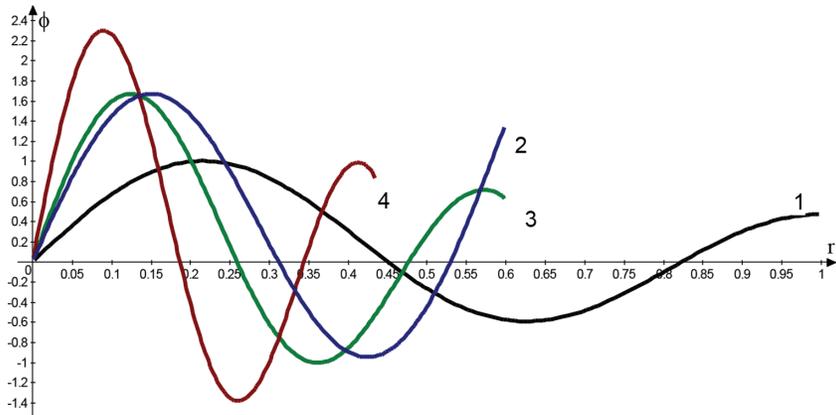
c) $\alpha = 1$. $m=3$

Figure 2: The radial wave profiles $m = 1, 2, 3$ for different non-dimensional liquid depths h_1 / R_1.
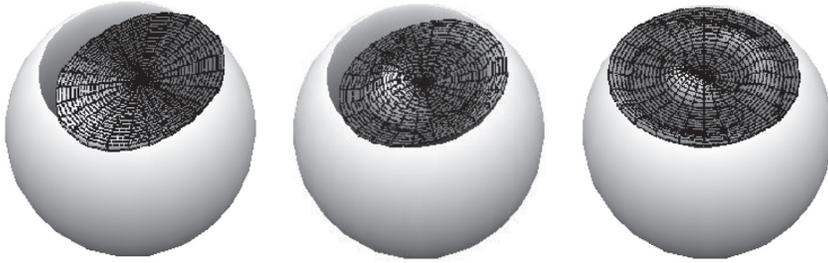
Figure 3: Spatial wave patterns for $a = 1$; $m = 1, 2, 3$.

Table 3: Sloshing frequencies of the fluid-filled spherical shell with baffles, Hz.

	ω^2/g		
m	$R_{int} = 1.0$ m	$R_{int} = 0.7$ m	$R_{int} = 0.2$ m
1	2.1232	2.0435	1.4234
2	5.9800	5.9723	5.8405
3	9.4789	9.4785	9.4567
4	12.9431	12.9430	12.9358
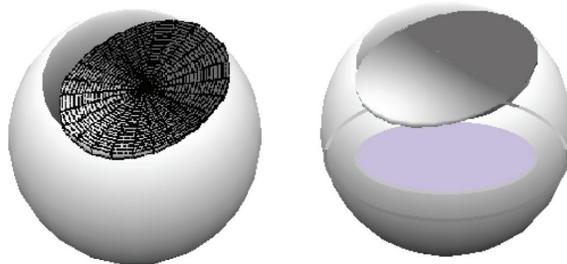
Figure 4: Spatial mode shapes for $a = 1$; $m = 1$ of un-baffled a) and baffled tanks b).

$0.5 < h_2 / R_1 < 2.39$. The inner radius R_{ir} of the ring free surface is defined by the dive level of the spherical shell z_s and the filling level h_2 as follows: $R_{ir} = \sqrt{R_1^2 - (h_2 - z_s)^2}$.

The results are illustrated in Fig. 5 for two lowest eigenvalues of the mode $a = 1$. Here numbers 1, 2 correspond to frequencies of cylindrical tanks with ring and circular free surfaces, respectively. If $h_2 = 0.5$ m, then both tanks have the complete circular free surfaces.

Figure 5a) and b) demonstrates changes in the first and second frequencies of the mode $a = 1$ via the filling level h_2. The values of frequencies increase significantly with increasing the inner radius of the ring free surface. The maximum values of frequencies correspond to $h_2 = z_s$; $R_{ir} = R_1$. Here we get the analogy with the "ice-fishing problem" for the spherical shell with $h_1/R_1 = 1.99$ (see Tables 1 and 2). Sloshing frequencies of cylindrical shell with circular free surface are stabilized when $h_2 > z_s$; one can observe here the typical monotonic
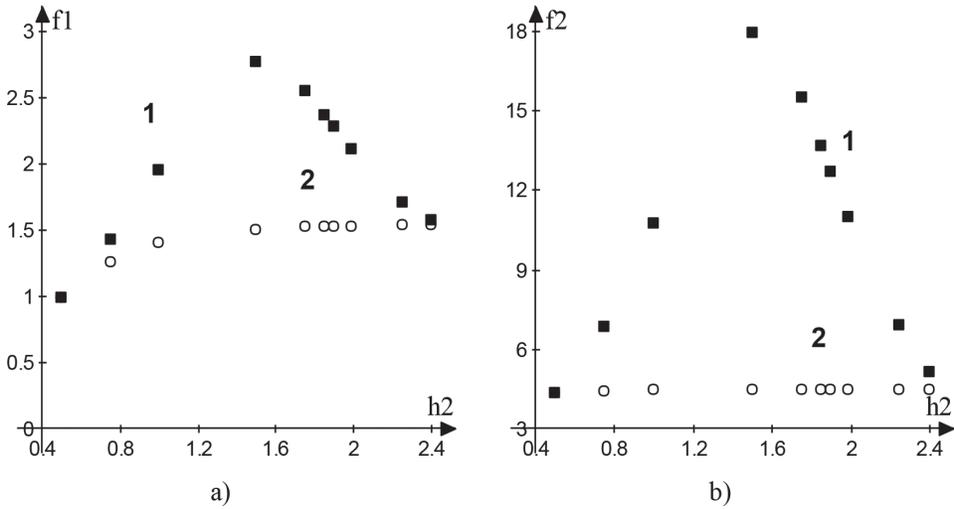
Figure 5: Frequencies of cylindrical shell with ring and circular free surfaces.

dependences. The benefit of a partly covered free surface is that it increases the natural frequencies.

4.3 Modes and frequencies of the empty cylindrical–spherical tank

Consider the elastic spherical-cylindrical tank without baffles (Fig. 1). The shell structure is clamped at the bottom edge. Natural frequencies Ω_k and modes $\mathbf{u}_k$, $k = \overline{1, N}$ of the shell structure without the liquid are calculated using FEM as it is proposed in Ref. [7]. The shell structure has the following dimensions: $R_1 = 1$ m, $R_2 = 1.2$ m, $z_s = 1.5$ m, $H = 2.0$ m, wall thickness $h = 0.025$ m; and material properties: Young's modulus $E = 2 \cdot 10^5$ MPa, Poisson's ratio $v = 0.3$, density $\rho_s = 2700$ kg/m³. Four modes of vibration are shown in Fig. 6.

The modes 6a) and 6b) correspond to the duplicate frequency $\Omega_1 = \Omega_2 = 4.6359$ Hz. This frequency is the lowest one of the mode $a = 1$. The axisymmetric mode 6c) corresponds to the frequency $\Omega_3 = 5.9312$ Hz, that is the lowest one of the mode $a = 0$. The axisymmetric mode 6d) corresponds to the frequency $\Omega_4 = 50.9721$ Hz.
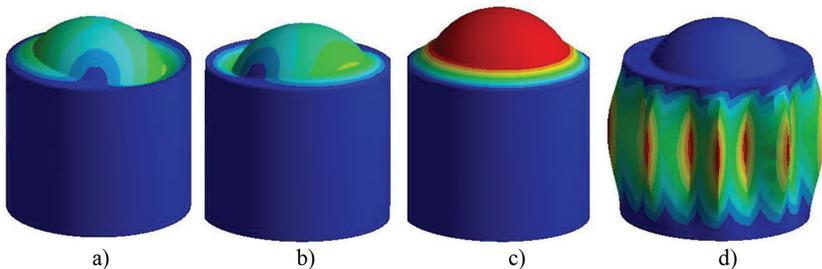
Figure 6: Modes of the empty cylindrical–spherical tank.

Table 4: Frequencies of the fluid-filled double tank, Hz.

m	ω	Dominant vibration	α
1	0.6223	Sphere sloshing	1
2,3	0.6359	Sphere wall	1
4	0.8294	Cylinder sloshing	1
5	0.9635	Sphere sloshing	0
22	5.0785	Cylinder wall	0

4.4 Modes and frequencies of the fluid-filled cylindrical–spherical tank

To define coupled modes of harmonic vibrations of the elastic tank, we represent the time-dependant unknown coefficients in series for potentials Φ_1, Φ_2, eqn (11), and for vibration modes **u** of the fluid-filled shell, eqn (5), in the form

$$c_k(t) = C_k e^{i\omega t}; \quad d_k(t) = D_k e^{i\omega t}, \tag{14}$$

where ω is an own frequency, C_k and D_k are unknown constants. Using (14) we obtain the eigenvalue problem for evaluating natural frequencies and modes of the fluid-filled cylindrical-spherical tank [9].

The filling levels are $h_1 = 1$ m and $h_2 = 1.5$ m. The lowest frequencies of the double tank are presented in Table 4.

The first frequencies are very close in value. For example, modes 1–5 have frequencies with difference within 1 Hz, and these modes are associated with different vibration types. The first twenty modes are predominantly sloshing ones.

5 CONCLUSIONS

The numerical procedure based on the coupling finite and boundary element methods is developed for the fluid-structure interaction analysis of the dual compartment tank. The considered problem has been solved using the multi-domain and single-domain boundary element approaches. The analysis demonstrates that sloshing and shell vibrations can not be considered separately. The lower frequencies of the fluid-filled tanks decrease to 0.2–0.4 and 0.1–0.6 of those of empty tanks for spherical and cylindrical compartments, respectively. The fluid-stricture interaction effects are more significant for the outer cylindrical part.

REFERENCES

[1] Brebbia, C.A, Telles, J.C.F. & Wrobel, L.C., *Boundary Element Techniques: Theory and Applications in Engineering*. Springer-Verlag: Berlin and New York, 1984.
[2] Wang, J. & Gao, X.W., Structural multi-scale boundary element method based on element subdivision technique. *Chinese Journal of Computational Mechanics*, **27**(2), pp. 258–263, 2010.

[3] Biswal, K.C., Bhattacharyya, S.K. & Sinha, P.K., Dynamic characteristics of liquid filled rectangular tank with baffles. *IE (I) Journal-CV,* **84**, pp. 145–148, 2004.

[4] Kumar, A. & Sinhamahapatra K.P., Dynamics of rectangular tank with perforated vertical baffle. *Ocean Engineering,* **126**(1), pp. 384–401, 2016.
https://doi.org/10.1016/j.oceaneng.2016.09.012

[5] Faltinsen, O.M. & Timokha, A.N., *Sloshing*. Cambridge University Press, Cambridge, 2009.

[6] Curadelli, O., Ambrosini, D., Mirasso, A. & Amani, M., Resonant frequencies in an elevated spherical container partially filled with water: FEM and measurement. *Journal of Fluids and Structures*, **26**(1), pp. 148–159, 2010.
https://doi.org/10.1016/j.jfluidstructs.2009.10.002

[7] Ravnik, J., Strelnikova, E., Gnitko V., Degtyarev, K. & Ogorodnyk,U., BEM and FEM analysis of fluid-structure interaction in a double tank. *Engineering Analysis with Boundary Elements*, **67**, pp. 13–25, 2016.
https://doi.org/10.1016/j.enganabound.2016.02.006

[8] Wan, F.Y.M. & Weinitschke, H.J., On shells of revolution with Love-Kirchoff hypothesis. *Journal of Engineering Mathematics*, **22**, pp. 285–334, 1988.
https://doi.org/10.1007/bf00058512

[9] Degtyarev, K., Glushich, P., Gnitko, V. & Strelnikova, E., Numerical simulation of free liquid-induced vibrations in elastic shells. *International Journal of Modern Physics and Applications,* **1**(4), pp. 159–168, 2015.

[10] Gnitko, V., Naumenko, V., Rozova, L. & Strelnikova, E., Multi-domain boundary element method for liquid sloshing analysis of tanks with baffles. *Journal of Basic and Applied Research International*, **17**(1), pp. 75–87, 2016.

[11] Gnitko, V., Degtyariov, K., Naumenko, V. & Strelnikova, E., BEM and FEM analysis of the fluid-structure Interaction in tanks with baffles. *International Journal of Computational Methods and Experimental Measurements*, **5**(3), pp. 317–328, 2017.
https://doi.org/10.2495/cmem-v5-n3-317-328

[12] McIver, P., Sloshing frequencies for cylindrical and spherical containers filled to an arbitrary depth. *Journal of Fluid Mechanics*, **201**, pp. 243, 1989.
https://doi.org/10.1017/s0022112089000923

[13] Faltinsen, O.M. & Timokha, A.N., Analytically approximate natural sloshing modes for a spherical tank shape. *Journal of Fluid Mechanics*, **703**, pp. 391–401, 2012.
https://doi.org/10.1017/jfm.2012.237

[14] Kulczycki, T., Kwaśnicki, M. & Siudeja, B., The shape of the fundamental sloshing mode in axisymmetric containers. *Journal of Engineering Mathematics*, **99**(1), pp. 157–193, 2016.
https://doi.org/10.1007/s10665-015-9826-6